JOURNAL OF FORENSIC SCIENCES

J Forensic Sci, November 2009, Vol. 54, No. 6
doi: 10.1111/j.1556-4029.2009.01170.x
Available online at: interscience.wiley.com

TECHNICAL NOTE

Diego Gonzalez-Aguilera,[1] *Ph.D. and Javier Gomez-Lahoz,*[1] *Ph.D.*

Forensic Terrestrial Photogrammetry from a Single Image

ABSTRACT: Forensic terrestrial photogrammetry is one of the most valuable and low-cost resources of spatial data available today. Due to the ephemeral crime scene characteristics, these photographs can often capture information that is never to be seen again. This paper presents a novelty approach for the documentation, analysis, and visualization of crime scenes for which only a single perspective image is available. The photogrammetric process consists of a few well-known steps in close-range photogrammetry: features extraction, vanishing points computation, camera self-calibration, 3D metric reconstruction, dimensional analysis, and interactive visualization. Likewise, the method incorporates a quality control of the different steps accomplished sequentially. As a result, several cases of study are presented in the experimental results section in order to test their viability. The full approach can be applied easily through the free software, sv3DVision, which has been evaluated by a number of police officers, forensic scientists, and forensic educators satisfactorily.

KEYWORDS: forensic science, crime scene, geomatic engineering, close-range photogrammetry, computer vision, software development

One of the primary goals of forensic photogrammetric analysis is to generate metric data for presentation in court. Techniques for analyzing nonmetric terrestrial images can be grouped in two main categories: the classical stereo-pair (solved with collinearity condition) and the popular oblique and convergent multiphoto (solved with collinearity condition and bundle adjustment equations). Forensic cases that have multiple images taken at convergent angles can proceed much like other standard close-range photogrammetric projects exploiting their advantages from the greater redundancy in the solutions (if good camera angles are available) so the solutions are usually stronger and more accurate to the measurements and drawings obtained which are not restricted to a 2D plane. The solution is obtained by a nonlinear least-squares bundle adjustment (1). The adjustment can carry camera interior orientation parameters and so further refinement (self-calibration) can be carried out. The adjustments can often be solved without control points using a free-network adjustment. On the other hand, when nonconvergent images are available, stereo-based photogrammetric approaches can be used. In this case, it is advisable to use calibrated and known cameras. The basic method of determining camera orientation from control points is called resection. The resection is commonly solved using the collinearity equations in a least-square solution—one aspect of bundle adjustment. The mathematical method used to solve the nonlinear bundle solution, like most nonlinear solution methods, requires approximate values to start. These surveys require to establish the geometry of stereo-pair carefully, especially the base and distance to the object. In addition, the angles of the camera cannot be forced at all so the camera axis is horizontal. In this context, particular interest has those cases in which a complete analysis with the minimum amount of external information (such as field surveys or camera calibration) is required. In fact, photogrammetric analysis in forensics is often characterized by a lack of information. The forensic analyst is often confronted with a single image of an unknown scene taken with an unknown camera. Under these conditions it is really difficult if not impossible to get useful information. With the aim of dealing with this scope, in this paper, from a single image and based on vanishing points geometry, a semiautomatic 3D reconstruction is provided by analytical and geometric methods, some of them incorporating novel and robust approaches. In addition, a software package "sv3DVision" has been developed providing a flexible and easy-to-use environment, even by practitioners who are not experts in photogrammetry. Earlier work in this area has been tested by the authors (2), where a preliminary approach based on a dimensional analysis is presented.

The paper presents the following layout and organization: after this introduction, Section 2 outlines the geomatic approaches dedicated for 3D crime scene recording and reconstruction. Section 3 explains in detail the full photogrammetric process developed using a single image. Section 4 shows some experimental results applied to simulated crime scenes. A final section is devoted to give some conclusions.

Geomatic Approaches for Crime Scene Recording and Reconstruction

There are several application areas in which geomatic engineering is often necessary, especially those where no original measurements are available. In this sense, geomatic technologies provide several approaches to get the knowledge of shapes and thus determine characteristic metric quantities such as distances, coordinates, or surface areas. In relation to forensic casework and the crime scene recording and reconstruction, three main geomatic approaches depending on sensor's type can be outlined.

Approaches Based on Passive Sensors, Digital, and Video Cameras

A system which creates 3D surface models from a sequence of images taken with a hand-held video camera is presented (3). Images are acquired by the user moving the camera around the object. The camera motion is recovered by matching corner

[1]Department of Cartographic and Land Engineering, Salamanca University, 05003 Avila, Spain.

Received 5 May 2008; and in revised form 4 Dec. 2008; accepted 6 Dec. 2008.

features in the image sequence. Dense stereomatching is carried out between the successive frames. The input images are used as surface texture to produce photorealistic 3D models. However, it is a scaled version of the original object as the metric size cannot be recovered from sequences of monocular images. Monocular approaches do not work well for some critical motion sequences. A system called Instant Scene Modeler which uses stereo cameras to obtain 3D data, estimate camera motion, and register successive frames together is developed (4). The stereo camera approach allows free camera motion without any restrictions. The resulting models are fully calibrated (allow Euclidean measurement) and have photorealistic appearance. The data acquisition and processing takes minutes. Nevertheless, the accuracy of the system is not enough to meet the requirements of a crime scene reconstruction. More recently, Crime Scene Virtual Tour (5) provides a distinctive virtual reality solution for crime scene investigation and reconstruction, which is used to document and observe complete information of the crime scene. Based on 360° panoramic images, Crime Scene Virtual Tour is a multimedia tool which integrates panoramic crime scene images, still images, interactive map, slideshow, texts, audios, links, thumbnails, etc. It provides an easy way to reconstruct a 3D crime scene through images and offers unparalleled features to crime scene investigators, which takes them back to the crime scenes and enables them to wander through the scene. However, this platform does not support metric capabilities, thus a metric analysis of the crime scene could not be performed.

Approaches Based on Active Sensors, Terrestrial Laser Scanner

There are several laser-scanning approaches which incorporate new computer methods and even novel devices for forensic analysis. In relation to the first approach Vanezisa et al. (6) describes an approach for facial reconstruction using laser scanner and 3D computer graphics. Skull and facial data from living subjects are acquired using an optical laser scanning system. The resulting image can also be modified within an identikit system which allows the addition of facial features as appropriate. In relation with the second approach, Rusinkiewicz and Levoy (7) proposed a real-time handheld 3D model acquisition system that permits the user to rotate an object by hand and see a continuously updated model as the object is scanned. The advantage of this system is that the user can find and fill holes in the model in real time and determine when the object is completely covered. The disadvantage of this system is that it requires physical contact with the subject and specific and synchronized hardware. In the same context but applied over large scenes, Bahmutov et al. (8) describe an efficient and interactive system for modeling large-scale interior scenes. The system is based on the structured light technique following a custom approach of projecting a matrix of 11×11 laser spots in the field of view of a digital camera. The depth is calculated using multiple dense color and sparse depth frames which share the same center of projection. However, the resolution of the obtained geometry is not enough for the description of objects with high complexity.

Multisensor Approaches Based on Passive and Active Sensors

Some projects combine the imaging capabilities of a laser scanner and close-range photogrammetry to measure the scene. The authors present a method for bite mark identification based on the individuality of a dentition, which is used to match a bite mark to a suspected perpetrator (9). This matching is based on a tooth-by-tooth and arch-to-arch comparison utilizing parameters of size, shape, and alignment. While the most common method used to analyze bite marks is carried out in 2D space, this method presents a new 3D documentation, analysis, and visualization approach based on forensic 3D/computer-aided design supported photogrammetry, and the use of a 3D surface scanner. Based upon the 3D detailed representation of the cast with the 3D topographic characteristics of the teeth, the interaction with the 3D documented skin can be visualized and analyzed on the computer screen. The authors developed a multisensor approach for creating accurate virtual environments (10). This approach uses 3D range sensor data, multiple CCD cameras, and a color high-resolution digital still camera. However, the system is not very flexible and manageable, not being suited for the recording and reconstruction of crime scenes. The authors proposed the Model Cameras which is a low-cost hand-held scene modelling device (11). It consists of a digital video camera with 16 laser points attached to it. Model Camera acquires 16 depth samples per frame and registers the frames using depth and color information. The frames are merged together into a texture-mapped model. However, the surfaces are approximated with a few quadrics and the approach only works for smooth continuous surfaces.

Therefore, while the approaches based on active sensors (terrestrial laser scanner) remain expensive and require specific tools for processing range dataset, passive sensors (digital camera) remain the most complete, economical, portable, flexible, and widely used. However, sometimes it is not possible to obtain such images, mainly when we work in interior scenes and the overlap and coverage limitations are difficult to overcome. In addition, trying to reconstruct a crime scene through multiple convergent images sometimes requires time and patience in order to obtain good results.

In the present case, the developed approach represents a clear and novel alternative to the limitations remarked above, especially considering that only one image is enough for providing a geometric characterization of the crime scene. Particularly, the following aspects can be outlined:

- Digital amateur cameras can be used.
- Noncalibrated and even unknown cameras (that is, old photographs or paintings) could be analyzed.
- Easy-to-use for nonexperts in photogrammetry.
- Semi-automatic process.
- Low-cost alternative.
- Quality and reliability in the results with accuracies around 5 cm.

Photogrammetric Process

From a single image, it is possible to extract relevant metric information about the crime scene and even to reconstruct a 3D model. One of the most critical steps in this process appertains to identification, with a high precision and reliability, of its structural elements, specially vanishing lines and points. These elements constitute the framework that supports the whole process as they provide independent geometric constraints which can be exploited in several ways: from camera self-calibration and a dimensional analysis of the crime scene to its own 3D reconstruction and visualization (Fig. 1).

Image Analysis: Features Extraction

One of the most critical steps in the metric analysis from a single image resides in detecting with high precision and reliability

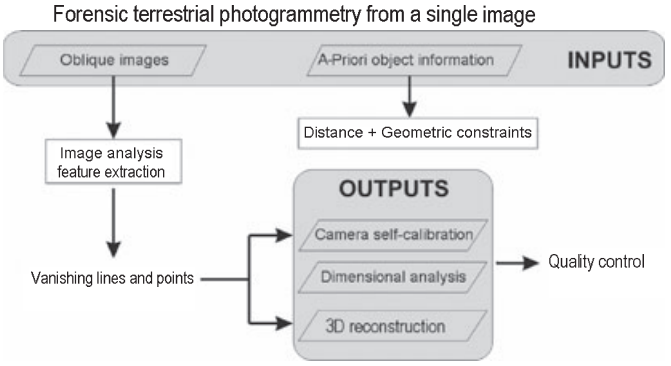

FIG. 1—*Forensic terrestrial photogrammetry from a single image.*

structural elements belonging to an oblique image. Man-made objects are often present in the crime scene, therefore features like straight lines and angles can be used to retrieve information about the camera or the 3D structure of the captured object. Nevertheless, this is not an easy task, taking into account that usually images contain noise due to their own acquisition process as well as the radial lens distortion. Thus, although several algorithms based on image processing exist currently, hierarchical and hybrid approaches will be required in order to guarantee quality. Unfortunately, a universal method for automatic vectorization does not exist, so it will be the own requirements of each case which will define and adapt the algorithm. In this context van den Heuvel (12) applies a line-growing algorithm called the Burns detector (13) for vanishing lines extraction; Tuytelaars et al. (14) created a parameter space based on Hough transform (15) to detect vanishing lines automatically; more recently the study (16–18) applied Canny filter (19) for the same purpose.

In this case and taking into account the methods remarked above, the developed approach (Fig. 2) is also based on line segments extraction but incorporates clustering strategies together with robust estimators that allow us to extract vanishing lines and points.

1. Straight line extraction combining Canny and Burns operators. This combination exhibits the following advantages compared with other alternatives: computational efficiency, high accuracy, and reliability in the localization of the edge points, and image noise does not degenerate its performance.
2. Clustering of segments analyzing the slope and distance between segments. This estimation is performed only with line segments that satisfy the orientation constraint. In this step, an estimation of radial lens distortion is also provided exploiting the presence of short segments (mini-segments) through collinearity condition.
3. Clustering of segments according to three main orthogonal directions of the scene or three vanishing points. This step is performed through a robust estimator, RANSAC (RANdom SAmple Consensus) (20), that incorporates slope analysis as a voting criterion, allowing detection of possible outliers (wrong vanishing lines) during the clustering process. Moreover, in order to provide more automatism and efficiency, an adaptative threshold and performance of the algorithm (21) has been developed.
4. Robust computation of vanishing points. The presence of mini-segments due to the automatism and the own weakness of the scene's geometry provide unfavorable intersection cases for

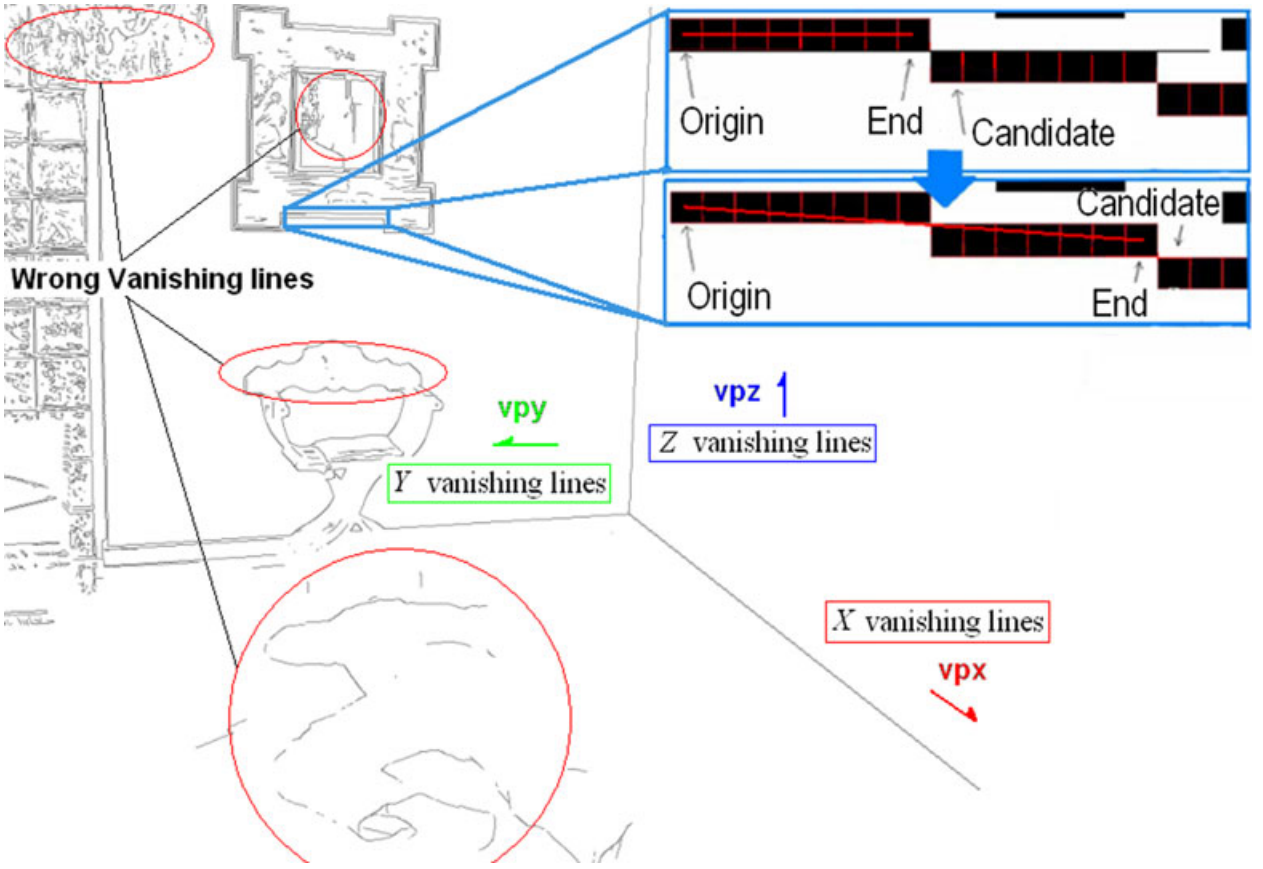

FIG. 2—*Image analysis: features extraction.*

vanishing points computation. Based on one of the most renowned methods, the Gaussian sphere (22), an original two-fold approach for vanishing points computation has been developed.

- An estimation step which inherits some of the analytical concepts of the traditional Gaussian sphere method combined with RANSAC.
- A computation step which applies a reweighted least square adjustment supported by modified Danish M-estimator (23).

More details about this original approach are described by Aguilera et al. (24).

Camera Self-Calibration

Camera calibration has been studied for many years and there are many methods available to find the parameters precisely. Although most existing methods require information of the known scene points and the use of multiple images, there are several calibration approaches exploiting the presence of vanishing points which have been reported in close-range photogrammetry (12,25,26) as well as in computer vision (16,27–29). In the context of close-range photogrammetry the general approach established is based on the use of three orthogonal vanishing points and some constraints among lines, while in the context of computer vision, several approaches are supported by the computation and decomposition of the absolute conic from three vanishing points or the rotation matrix.

The self-calibration method developed presented a hybrid character that combined approaches related to close-range photogrammetry and computer vision. On one hand, the present approach is similar in some ways to that proposed by Caprile and Torre (27) who exploited vanishing points geometry to recover the projection matrices directly, and on the other hand, the strategy used exploits simple properties of vanishing points adding some geometric constraints derived from image analysis step. Therefore, a complete camera model can be recovered following two steps in which internal and external parameters are estimated separately.

In the first step, the intrinsic parameters, that is, the focal length, the principal point, and the radial lens distortion, are recovered automatically based on vanishing points geometry and image analysis. The orthocenter of the triangle (Fig. 3) formed from the three vanishing points, *vp*, of the three mutually orthogonal directions identifies the principal point, pp, of the camera through the cross product of the segments of the triangle and its heights (Eq. 1). The focal length can be computed afterwards as the square root of the product of the distances from the principal point to any of the triangle's vertices and the opposite side.

$$\begin{aligned}(\mathrm{vpx}-\mathrm{pp})(\mathrm{vpy}-\mathrm{vpz})&=0\\(\mathrm{vpy}-\mathrm{pp})(\mathrm{vpx}-\mathrm{vpz})&=0\\(\mathrm{vpx}-\mathrm{pp})(\mathrm{vpz}-\mathrm{vpy})&=0\end{aligned}\qquad(1)$$

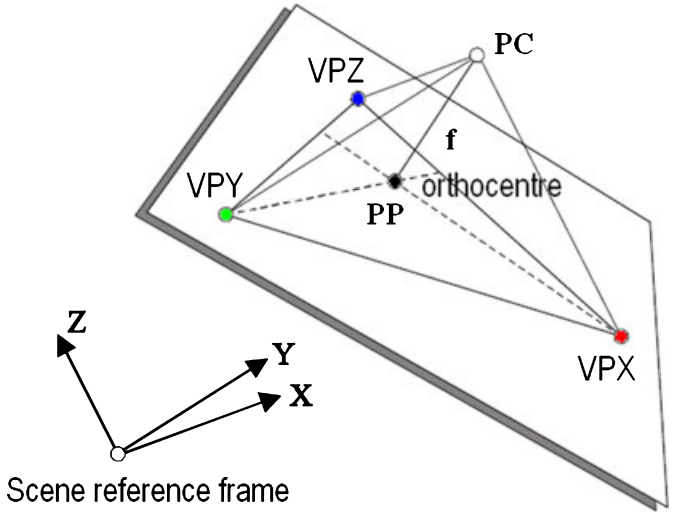

FIG. 3—*Intrinsic camera parameters from a single image.*

$$f=\sqrt{\left|\left(x_{vp}-x_{\mathrm{pp}}\right)\left(y_{vp}-x_{\mathrm{pp}}\right)+\left(x_{vp}-y_{\mathrm{pp}}\right)\left(y_{vp}-y_{\mathrm{pp}}\right)\right|}\qquad(2)$$

Finally, the radial lens distortion parameters (k_1,k_2) are estimated exploiting the presence of short segments (mini-segments) through collinearity condition. This estimation is performed only with line segments that satisfy the orientation constraint. For several mini-segments j with several points per segment i, the functional model proposed is as follows:

$$a_j x'_{ij}+b_j y'_{ij}+1\Big/\left(1+k_1\mathrm{dr}'^2_{ij}+k_2\mathrm{dr}'^4\right)=F=0\qquad(3)$$

where (a_j,b_j) are the normalized straight line parameters, (x_{ij},y_{ij}) are the straight line coordinates, dr is the radial distance, and (k_1,k_2) are radial lens distortion parameters.

In the second step, the extrinsic parameters, that is, the perspective rotation matrix and the translation vector which describe the rigid motion of the coordinate system fixed in the camera are estimated in a two-pass process. First, the rotation matrix (Eq. 4) (camera orientation) is obtained automatically based on the correspondence between the vanishing points and the three main crime scene directions. This relationship allows us to extract the cosine vectors of optical axis, obtaining directly the three angles (axis, tilt, and swing) (Eq. 5). This approach is really straightforward in comparison with other approaches such as RQ decomposition, for instance, and provides good results as long as vanishing points and internal camera parameters have been computed with high precision and reliability.

$$\begin{aligned}r_{11}&=\cos\left(\overline{x'x}\right)=\frac{x_{vpx}-x_{\mathrm{pp}}}{|\overline{pcvpx}|}\quad r_{12}=\cos\left(\overline{y'x}\right)=\frac{x_{vpy}-x_{\mathrm{pp}}}{|\overline{pcvpy}|}\quad r_{13}=\cos\left(\overline{z'x}\right)=\frac{x_{vpz}-x_{\mathrm{pp}}}{|\overline{pcvpz}|}\\r_{21}&=\cos\left(\overline{x'y}\right)=\frac{y_{vpx}-y_{\mathrm{pp}}}{|\overline{pcvpx}|}\quad r_{22}=\cos\left(\overline{y'y}\right)=\frac{y_{vpy}-y_{\mathrm{pp}}}{|\overline{pcvpy}|}\quad r_{23}=\cos\left(\overline{z'y}\right)=\frac{y_{vpz}-y_{\mathrm{pp}}}{|\overline{pcvpz}|}\\r_{31}&=\cos\left(\overline{x'z}\right)=\frac{-f}{|\overline{pcvpx}|}\quad r_{32}=\cos\left(\overline{y'z}\right)=\frac{-f}{|\overline{pcvpy}|}\quad r_{33}=\cos\left(\overline{z'z}\right)=\frac{-f}{|\overline{pcvpz}|}\end{aligned}\qquad(4)$$

$$\begin{array}{lll} axis = \text{arctg}(|r_{31}/r_{32}|) & tilt = \arccos(r_{33}) & swing = \text{arctg}(r_{13}/r_{23}) + 180^\circ \\ \text{where } 0^\circ \le axis \le 90^\circ & \text{where } 0^\circ \le tilt \le 180^\circ & \text{where } 90^\circ \le swing \le 270^\circ \end{array} \quad (5)$$

These rotation angles use the *axis*, *tilt*, and *swing* to describe the rotation of object-space to image-space coordinates. Particularly, the *axis* is a clockwise rotation about the object-space Z axis (nadir direction), and is the angle between the object-space Y-axis. The *tilt* angle is a rotation about a line parallel to the true horizon line, and is the angle between the principal ray (image plane normal) and the line from the principal point to the Z vanishing point. The *swing* angle is a rotation about the image z-axis and is the angle between the positive image y-axis and the trace of the projection of the principal plane (generated by the principal ray and the nadir direction) below the image x-axis (Fig. 4).

Then, the translation vector, **x**, that is, the absolute camera pose is estimated based on some *a priori* crime scene information, for example, a distance together with a geometric constraint defined by the user. For the estimation of **x**, the Gauss-Markov model of least squares is normally used:

$$\mathbf{v} = A\mathbf{x} - l.$$

$$A = \begin{bmatrix} r_{31}(x_i - x_{pp}) + r_{11}f & r_{32}(x_i - x_{pp}) + r_{12}f & r_{33}(x_i - x_{pp}) + r_{13}f \\ r_{31}(y_i - y_{pp}) + r_{21}f & r_{32}(y_i - y_{pp}) + r_{22}f & r_{33}(y_i - y_{pp}) + r_{23}f \end{bmatrix}$$

$$l = \begin{bmatrix} (x_i - x_{pp})(r_{31}X_i + r_{32}Y_i + r_{33}Z_i) + f(r_{11}X_i + r_{12}Y_i + r_{13}Z_i) \\ (y_i - y_{pp})(r_{31}X_i + r_{32}Y_i + r_{33}Z_i) + f(r_{21}X_i + r_{22}Y_i + r_{23}Z_i) \end{bmatrix} \quad (6)$$

where r_{ij}'s are the 3×3 rotation matrix elements, f, the focal length, x_{pp}, y_{pp}, the principal point coordinates, and X_i, Y_i, Z_i constitutes *a priori* known information about the crime scene.

Therefore, the reference frame for the camera pose estimation is defined with relation to the crime scene geometry based on a local coordinate system. The robustness of the method depends on the precision and reliability of vanishing points computation, so the incorporation of robust estimators in the previous step is crucial.

Dimensional Analysis

Once the camera model has been estimated, a dimensional analysis of the crime scene based on distances, angles, and areas could be performed. Moreover, this step constitutes a possible validation of the accuracy of the reconstructed model taking into account that the results have been compared with other surveying measurements, such as expeditious topography and terrestrial laser scanner. Particularly, the scene coordinates of a point P are usually recovered by means of the collinearity model. The collinearity condition states that a point in scene space, its corresponding point in an image, and the projective center of the camera lie on a straight line:

$$\begin{aligned} X &= X_0 + (Z - Z_0) \cdot \frac{r_{11}(x - x_{pp}) + r_{12}(y - y_{pp}) - r_{13}f}{r_{31}(x - x_{pp}) + r_{32}(y - y_{pp}) - r_{33}f} \\ Y &= Y_0 + (Z - Z_0) \cdot \frac{r_{21}(x - x_{pp}) + r_{22}(y - y_{pp}) - r_{23}f}{r_{31}(x - x_{pp}) + r_{32}(y - y_{pp}) - r_{33}f} \end{aligned} \quad (7)$$

that relates the image measurements to the object coordinate system (X,Y,Z) only through the camera constant f, the image coordinates (x,y), the principal point (x_{pp},y_{pp}), the projective center (X_0,Y_0,Z_0), and the rotation matrix **R** that renders the misalignment of both reference frames.

The scene distance L can be expressed as:

$$L_{12}^2 = (X_1 - X_2)^2 + (Y_1 - Y_2)^2 + (Z_1 - Z_2)^2 \quad (8)$$

where X, Y, and Z are the coordinates obtained from a single image at the crime scene.

In relation to object area computation, the triangle semiperimeter formula is used:

$$\text{Area}_{XZ} = \sum_{i=1}^{n} \left| \sqrt{SP_{XZi} \cdot (SP_{XZi} - L_{12}) \cdot (SP_{XZi} - L_{23}) \cdot (SP_{XZi} - L_{31})} \right|$$
$$SP_{XZi} = (L_{12} + L_{23} + L_{31})/2 \quad (9)$$

where SP is the semiperimeter of each triangle i that defines the area.

Finally, with relation to angles, for a triangle in the Euclidean plane with edges a, b, c and opposite angles α, β, γ, the following holds:

$$\begin{aligned} a^2 &= b^2 + c^2 - 2bc\cos\alpha; b^2 = a^2 + c^2 - 2ac\cos\beta \\ c^2 &= a^2 + b^2 - 2ab\cos\gamma \end{aligned} \quad (10)$$

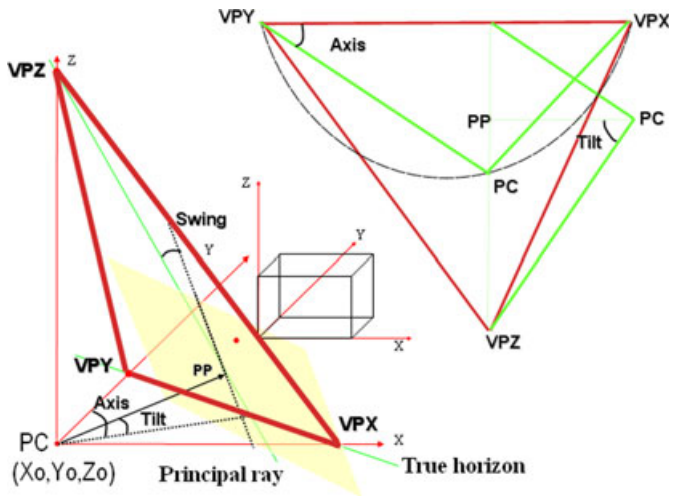

FIG. 4—*Extrinsic camera parameters from a single image.*

3D Reconstruction and Visualization

From a single image alone it is not possible to provide a 3D reconstruction of the crime scene. Equation (7) draws attention to the fact that because the Z coordinates are on the right hand side, to each image point there are infinitely many possible object points. To do so one also needs either a second image of the same scene taken from a different place or additional information about the object (for example, geometric constraints and image invariants). For crime scenes, geometric constraints on the objects (perpendicularity, coplanarity, parallelism, and so on) and image invariants (distances and angles) can be used to solve the 3D reconstruction problem from a single image (Fig. 5).

Therefore, the whole 3D reconstruction problem could be reduced to the problem of computing the coordinates of the scene

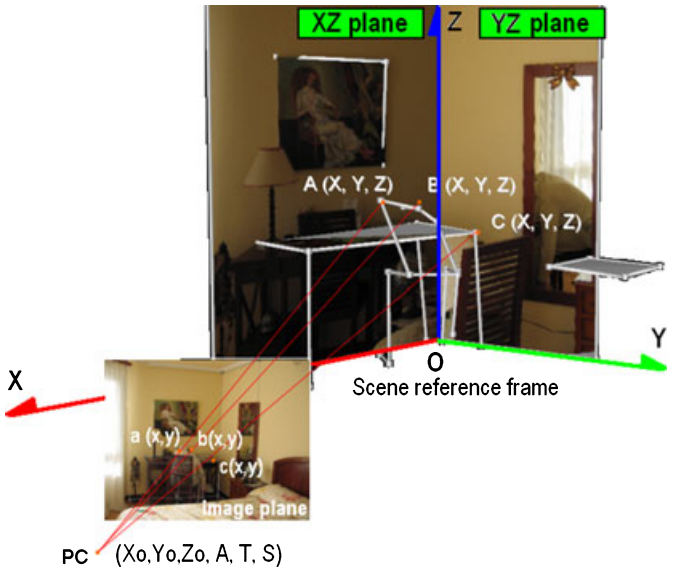

FIG. 5—*3D reconstruction from a single image based on geometric constraints and image invariants.*

through the collinearity condition (7) augmented by geometric constraints to render the fact that the object points lie on parallel planes to the reference frame defined during camera pose estimation (that is, $X = \pm K$; $Y = \pm K$; $Z = \pm K$ where K is a constant). As a result, every dimension value calculated through this approach must be parallel to one of the major planes (*XZ*, *YZ*, and *XY*).

Finally, the visualization of a 3D scene is often the only product of interest for the external world and remains the only possible contact with the scene. Furthermore, an interactive visualization of the crime scene enables us to obtain impossible views and perspectives that exploit its analysis capabilities, so a realistic and accurate visualization is often required. The Virtual Reality Modelling Language (VRML) format is the standard chosen to provide an interactive visualization of the results guaranteeing flexibility and scalability in the visualization at the same time, so different 3D models can be incorporated and managed easily. In this way, an automatic transformation of the reconstructed crime scene into a topological structure (points, lines, and surfaces), sorted hierarchically in nodes network is performed, allowing three different levels of visualization: wireframe, shaded, and textured. Materials defined by their colors and radiometric properties (opaqueness, transparency, diffusion, reflection, and emission) or rectified textures are mapped through a uniform and continuous rendering supported internally by VRML. Last but not least, using the virtual reality model provided by VRML, a virtual camera can then be placed in the 3D model of the scene looking at the model from whatever impossible position with the aim of improving the analysis capabilities.

Quality Control: Error Estimation

Finally, considering that the whole photogrammetric process developed involves many steps, one of the most difficult issues is the estimation of the measuring precision together with the probability of these measurements (confidence intervals). There are several factors that particularly contribute to the variation and thus to the error propagation:

- Automatic features extraction process which includes lines and vanishing points.
- Estimation of internal camera parameters, especially the radial lens distortion.
- Estimation of external camera parameters, concretely the camera poses which requires that the operator introduces *a priori* known information about the scene.
- Identification and measurement of objects in the images by the operator.

The uncertainty of the measurements has been taken into account and a final statistical analysis has been performed based on error propagation. The evaluation of the results considers the parameters covariance matrix $\mathbf{C}_{pp}$ following the approach described by Mikhail and Ackermann (30):

$$\mathbf{Q}_{pp} = \left(\mathbf{A}^T\mathbf{W}\mathbf{A}\right)^{-1}$$
$$\mathbf{C}_{pp} = \sigma_0^2\mathbf{Q}_{pp} \tag{11}$$

where $\mathbf{A}$ is the design matrix, $\mathbf{Q}_{pp}$ is the parameters cofactor matrix, $\mathbf{W}$ is the weight matrix, $\sigma^2{}_0$ is the *a posteriori* variance of the adjustment, and $\mathbf{C}_{pp}$ is the covariance matrix of the estimated parameters.

On the other hand, in order to know the value of the method for forensic work, the confidence intervals of the measurements have been estimated. In addition, with the aim of reducing variation due to operator, each measurement has been obtained by three different operators and has been measured 10 times. Besides this, reference measurements obtained at the real site with a measuring tape (case study 1) and a laser scanner (case study 2) are used. As a result, the confidence intervals for each measurement are estimated considering the following: let n be the number of times each distance or surface area is measured (10 times for each of the three operators), let δ_i be the averaged discrepancy between reference measurement (K_i) and the averaged operator measurement (M_i), let $S_{\delta i}$ be the standard deviation of the discrepancies. As the number of measurements is limited in each case study, the results are in terms of the Student's t distribution. In this sense, let $0 < \alpha < 1$, and let $t_{n-1,1-\alpha/2}$ be the $1 - \alpha/2$ percentile of the Student's t distribution with $n - 1$ degrees of freedom. Then given M_i and the discrepancies δ_i, a $100(1 - \alpha)\%$ confidence interval for K_i is given through the following formula:

$$|K_i - (M_i + \delta_i)| \leq \left(1 + n^{-1}\right)^{1/2} S_{\delta i} t_{n-1,1-\alpha/2} \tag{12}$$

Experimental Results

In order to determine the quality, limitations, and advantages of this forensic photogrammetric approach, several case studies were analyzed for which only one image remained. Then, two of these cases corresponding to simulated crime scenes were reported. The criterions of choice of these two cases were based on showing the best and worst situations in which a successful solution could be provided.

Case Study 1: Unfavorable Case

Problem and Goal—This first case study represents a challenging test for the forensic terrestrial photogrammetry as it is characterized by a lack of information. Camera information is completely unknown and the geometry of the scene is complex due to the presence of free-form shapes and small details (as for example, lamps, armchairs, curtains, and so on). The main goal is focused in providing a dimensional analysis and 3D reconstruction from an unknown camera image. As a result, a digital archive could be

created from a single image performing as a basic technical assistance.

Methodology and Results—The input image (3008 × 2000 pixels) was analyzed semiautomatically to extract basic features such as vanishing lines and vanishing points (Fig. 6). The input parameters (slope, orthogonal distance, and minimum length of edges) set up for this case were established manually especially for the clustering process due to the presence of free-form shapes and small details.

Table 1 shows the statistics obtained through the features' extraction process. It is important to remark that the number of wrong vanishing lines detected (outliers) reached 5%.

Next, a robust vanishing points computation was applied to guarantee more precision and reliability in the process. In this case, the own automatism in the features extraction led to the presence of mini-segments and thus an unfavorable intersection case for the vanishing points computation. Table 2 shows the results (coordinates and standard deviations) obtained in vanishing points computation once the robust estimators (RANSAC and Danish) have been

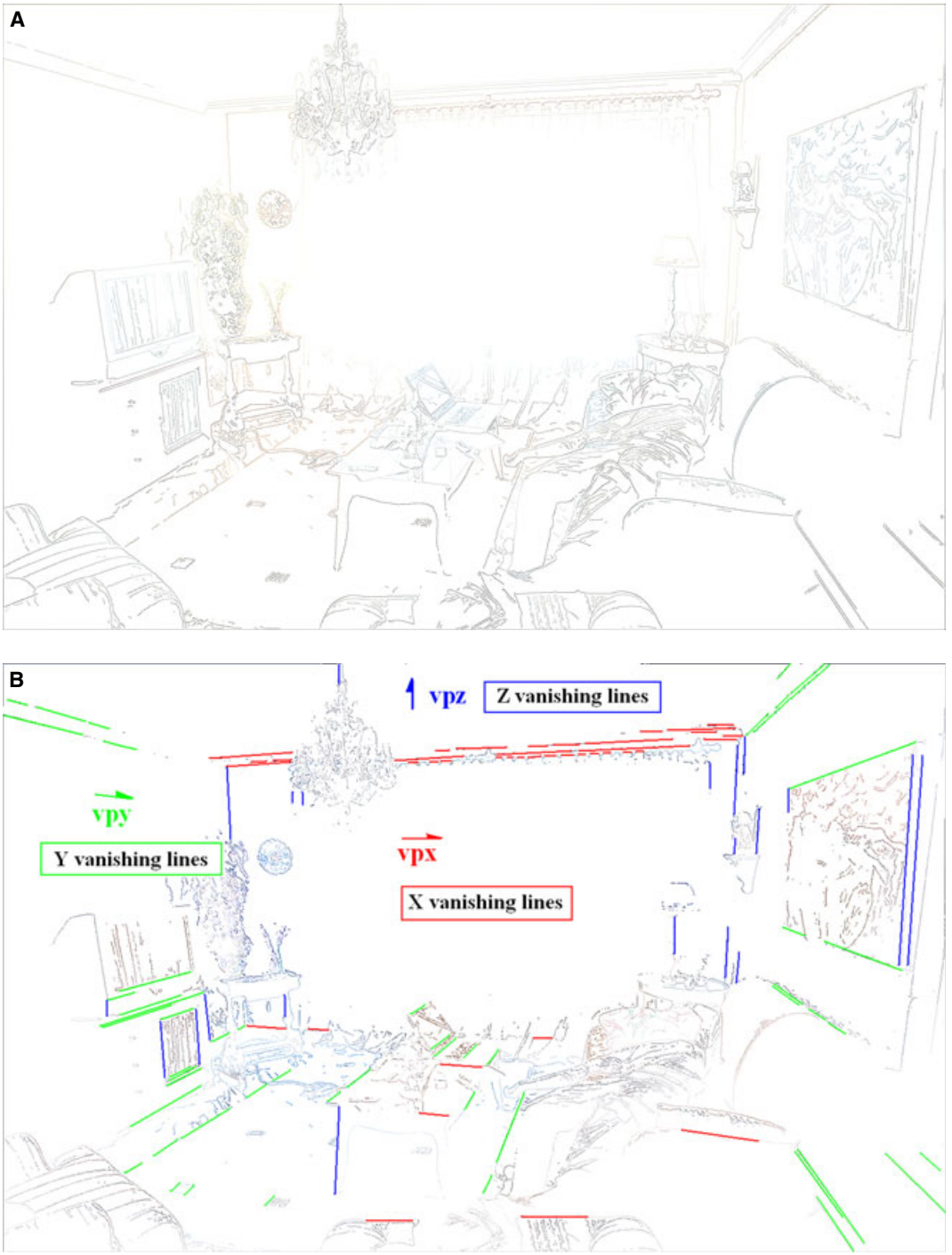

FIG. 6—*Case study 1: (A). Semi-automatic straight line extraction: Canny + Burns. (B). Semi-automatic clustering of vanishing lines according to the main directions of the crime scene (X,Y,Z).*

applied. A total of six iterations were required to achieve the convergence of the adjustment with a subpixel precision in vanishing points coordinates.

Afterwards, with the structural support of the crime scene provided by vanishing lines and points, an estimation of internal and external camera parameters was obtained based on *a priori* scene information (Table 3). A known distance (2.402 m) was introduced manually (Fig. 7). This distance which was considered free of error (because it was estimated with millimetric accuracy) was provided by the forensic officers using a measuring tape. Standard deviations of 2 cm and 0.5° were obtained for camera pose and camera orientation, respectively.

Finally, a dimensional analysis and 3D reconstruction (Fig. 7) exploiting the collinearity condition together with geometric constraints was performed by three different operators to reduce variation due to human factor. In relation to geometric constraints, these were forced to lie on planes parallel to the reference frame defined during camera pose estimation.

Some of the results of the dimensional analysis performed by three different operators, their means, and discrepancies together with the standard deviations and confidence intervals for each measurement are displayed in Tables 4 and 5. Discrepancies were obtained comparing the averaged measurements provided by the operators with reference measurements surveyed by forensic officers using a measuring tape.

In relation to the first distance analyzed (L_1) and based on the outcomes in Table 5, the mean measured distance (M_{L1}) was

TABLE 1—*Case study 1: statistics of features extraction.*

Vanishing Lines	55 segments clustered in *X* direction 77 segments clustered in *Y* direction 34 segments clustered in *Z* direction 8 segments clustered as "outliers"

TABLE 2—*Case study 1: robust vanishing points computation in pixels.*

Interpretation Planes + RANSAC: 1° Iteration Triangle AM + Danish Estimator: 2°–6° Iteration	vpx	vpy	vpz
x	−7574.5	1905.1	1395.5
y	850.7	701.1	10520.3
σ_{xx}	0	0.1	0
σ_{yy}	0.1	0.1	0.1

RANSAC, random sample consensus; AM, area minimization.

TABLE 3—*Case study 1: internal and external camera parameters and deviations.*

Internal Parameters (Units: mm)		External Parameters (Units: Degrees, m)	
pp [x] (mm)	11.6	Axis: 15.35°	X: 2.94
pp [y] (mm)	7.5	Tilt: 75.71°	Y: 5.79
f (mm)	14.1	Swing: 179.09°	Z: 1.5
k_1	0.00410		
k_2	−0.00001		
σ_{pp} [x]	0.2	σ_{Axis}: 0.4°	σ_X: 0.01
σ_{pp} [y]	0.3	σ_{Tilt}: 0.2°	σ_Y: 0.01
σ_f	0.3	σ_{Swing}: 0.06°	σ_Z: 0.02
σ_{k1}	0.00011		
σ_{k2}	0.0000021		

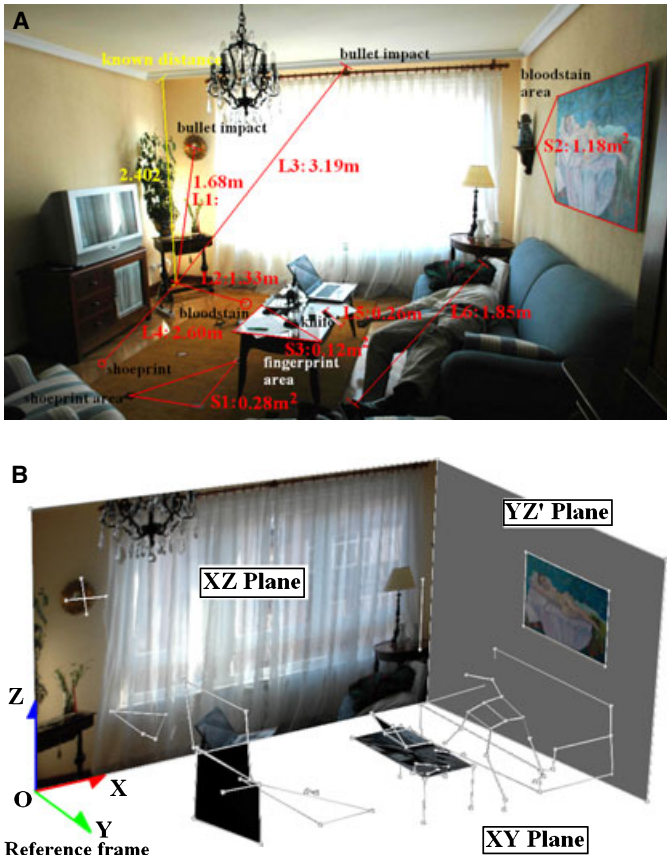

FIG. 7—*Case study 1. (A). Dimensional analysis. Measurements in meters averaged over each operator's measurements. (B). 3D reconstruction and visualization.*

1.68 m. For the test measurements of distances, the mean measured discrepancy (δ_{L1}) was 0.02 m higher than the reference distance (K_{L1}), with a standard deviation ($S_{\delta L1}$) of 0.01 m. Hence, an approximation of the reference measurement was given by 1.68 − 0.02 = 1.66 m with a certain confidence band. Considering the mean discrepancy, the standard deviation as well as the percentile points of the Student's t distribution, the width of the band, determined by the equation (12) was $t_{30-1,1-0.025} = t_{29,0.975} = 2.0452$. As a result, a 95% confidence interval for K_{L1} is given through the following formula:

$$|K_{L1} - (M_{L1} + \delta_{L1})| \leq 2.0452\left(1 + 30^{-1}\right)^{1/2} S_{\delta L1} = 0.02$$

TABLE 4—*Case study 1: dimensional analysis performed by three different operators measuring each dimension 10 times.*

Operator Test Distances (m)	1 Mean Measured Distance	2 Mean Measured Distance	3 Mean Measured Distance
$L1$	1.68	1.68	1.69
$L2$	1.33	1.34	1.33
$L3$	3.18	3.20	3.18
$L4$	2.59	2.60	2.61
$L5$	0.25	0.27	0.26
$L6$	1.85	1.88	1.86
Test areas (m^2)			
$S1$	0.28	0.29	0.27
$S2$	1.17	1.19	1.18
$S3$	0.11	0.13	0.12

TABLE 5—*Case study 1: reference measurements, mean measurements, their discrepancies, standard deviations, and confidence intervals, in meters.*

Reference Distances		Mean Measured Distances	Mean Discrepancies	Standard Deviation	Confidence Intervals
Test Distances (m)					
L1	1.66	1.68	$\delta'_{L1} = -0.02$	$S_{\delta L1} = 0.01$	(1.64, 1.68)
L2	1.31	1.33	$\delta'_{L2} = -0.02$	$S_{\delta L2} = 0.01$	(1.29, 1.33)
L3	3.16	3.19	$\delta'_{L3} = -0.03$	$S_{\delta L3} = 0.02$	(3.12, 3.20)
L4	2.57	2.60	$\delta'_{L4} = -0.03$	$S_{\delta L4} = 0.02$	(2.53, 2.61)
L5	0.23	0.26	$\delta'_{L5} = -0.03$	$S_{\delta L5} = 0.02$	(0.19, 0.30)
L6	1.81	1.85	$\delta'_{L6} = -0.04$	$S_{\delta L6} = 0.03$	(1.75, 1.87)
Reference Areas		Mean Measured Areas	Mean Discrepancies	Standard Deviation	Confidence Intervals
Test areas (m^2)					
S1	0.25	0.28	$\delta'_{S1} = -0.03$	$S_{\delta S1} = 0.02$	(0.21, 0.29)
S2	1.13	1.18	$\delta'_{S2} = -0.05$	$S_{\delta S2} = 0.03$	(1.07, 1.19)
S3	0.08	0.12	$\delta'_{S3} = -0.04$	$S_{\delta S3} = 0.03$	(0.02, 0.14)

This meant that the actual measured distance L_1 of the crime scene, with a 95% confidence was contained in the interval:

$$(1.66 - 0.02, 1.66 + 0.02 \text{ m}) = (1.64, 1.68 \text{ m})$$

Considering that the reference measured distance (K_{L1}) obtained with a measurement tape was 1.66 m, the mean measured distance (M_{L1}) obtained by operators, 1.68 m, could be considered correct with a significance level of 95%.

Considerations—This first experiment represents a clear contribution to forensic terrestrial photogrammetry activity, making easy a survey of the crime scene when only one image remains and relevant camera information is completely unknown. The final average discrepancy is around 0.03 m, which can be considered very acceptable taking into account the lack of camera information, mainly the unknown internal camera parameters (focal length, principal point, and radial lens distortion). Finally, special attention should be paid in the measurement L_6 which contains a higher standard deviation due to the particular interpretation of head and feet in the image by the operators.

Case Study 2: Favorable Case

Problem and Goal—This second case study shows the maximum possibilities of success in the metric analysis of a crime scene from a single image, because the camera, Nikon D70 (Nikon Hong Kong Ltd., Taikoo Shing, Hong Kong), has been previously calibrated on a laboratory using a planar target array. In this sense, the main goal is focused on asserting that the results obtained from a single image can be even better if the internal camera parameters are calibrated.

Methodology and Results—The methodology applied in this second experiment was more efficient because the internal camera parameters were known and the scene geometry was favorable. In this sense, the simulated crime scene image (3008×2000 pixels) was analyzed to automatically extract basic features (Fig. 8) such as vanishing lines and points. The input parameters (slope, orthogonal distance, and minimum length of edges) set up for these cases were established automatically. In addition, the robust vanishing point computation described previously was applied to guarantee more precision and reliability in the process.

Table 6 shows the statistics obtained through the features' extraction process as well as the vanishing points coordinates. In this case, the number of wrong vanishing lines detected (outliers) was lower than the case before and only reached 3%. In addition, due to the favorable perspective of the image only two iterations were required to obtain subpixel precision.

Afterwards, a first approximation for the partly known camera model was recovered semiautomatically. The known internal camera parameters were used to improve and check the results obtained automatically, while some manual interaction was required to retrieve camera pose (Table 7). A known distance (2.570 m) was introduced manually (Fig. 7). This distance was provided by the forensic officers using a terrestrial laser scanner, Trimble GX200. Standard deviations of 1 cm and 0.3° were obtained for camera pose and camera orientation respectively.

Finally, a dimensional analysis based on distances and surface areas which exploited the collinearity condition augmented by geometric constraints was performed together with a 3D reconstruction of the crime scene. In particular, all measurements must lie on the principal planes of the scene, that is, *XZ*, *YZ*, and *XY*. These planes constitute the reference frame established during camera pose estimation. Figure 9 shows the 3D crime scene reconstruction where a metric analysis based on distances and surface areas has been tested.

Some of the results of the dimensional analysis performed by three different operators, their means and discrepancies together with the standard deviations and confidence intervals for each measurement are displayed in Tables 8 and 9. These discrepancies were obtained by comparing the averaged measurements provided by the operators with the reference measurements surveyed with a terrestrial laser scanner, Trimble GX200 (Trimble Tempe, Tempe, AZ).

Now, trying to provide a detailed analysis of the surface areas and using the outcomes in Table 9, for the first measured surface area (S_1), its mean measured surface (M_{S1}) is 2.70 m^2, its mean measured discrepancy (δ_{S1}) is 0.02 m^2 higher than the reference surface area (K_{S1}) with a standard deviation ($S_{\delta S1}$) of 0.01 m^2. Hence, an approximation of the reference measurement was given by 2.70 m^2 − 0.02 m^2 = 2.68 m^2 with a certain confidence band. Considering the mean discrepancy, the standard deviation as well as the percentile points of the Student's t distribution, the width of the band, determined by the equation (12) was $t_{30-1,1-0.025} = t_{29,0.975} = 2.0452$. As a result, with 95% confidence:

$$|K_{S1} - (M_{S1} + \delta_{S1})| \leq 2.0452\left(1 + 30^{-1}\right)^{1/2} S_{\delta S1} = 0.04\,\text{m}^2$$

This meant that the actual measured surface S_1 of the crime scene, with a 95% confidence was contained in the interval:

$$(2.68 - 0.04, 2.68 + 0.04 \text{ m}^2) = (2.64, 2.72 \text{ m}^2)$$

Considering that the reference measured surface area (K_{S1}) obtained with a terrestrial laser scanner was 2.68 m^2, the mean measured surface area (M_{S1}) obtained by operators, 2.70 m^2 could be considered valid with a significance level of 95%.

Considerations—This second experiment represented a favorable case because two main conditions were fulfilled: the perspective is good in the three main axis directions of the crime scene and the camera has been previously calibrated. In this sense, a high level of automation was obtained and thus the different thresholds of the process (slope, orthogonal distance, and minimum length of edges) was established automatically. The dimensional analysis and 3D reconstruction was compared with laser scanning. Particularly, several control points corresponding to the distances analyzed were measured using a terrestrial laser scanner, TrimbleGX200. A spatial

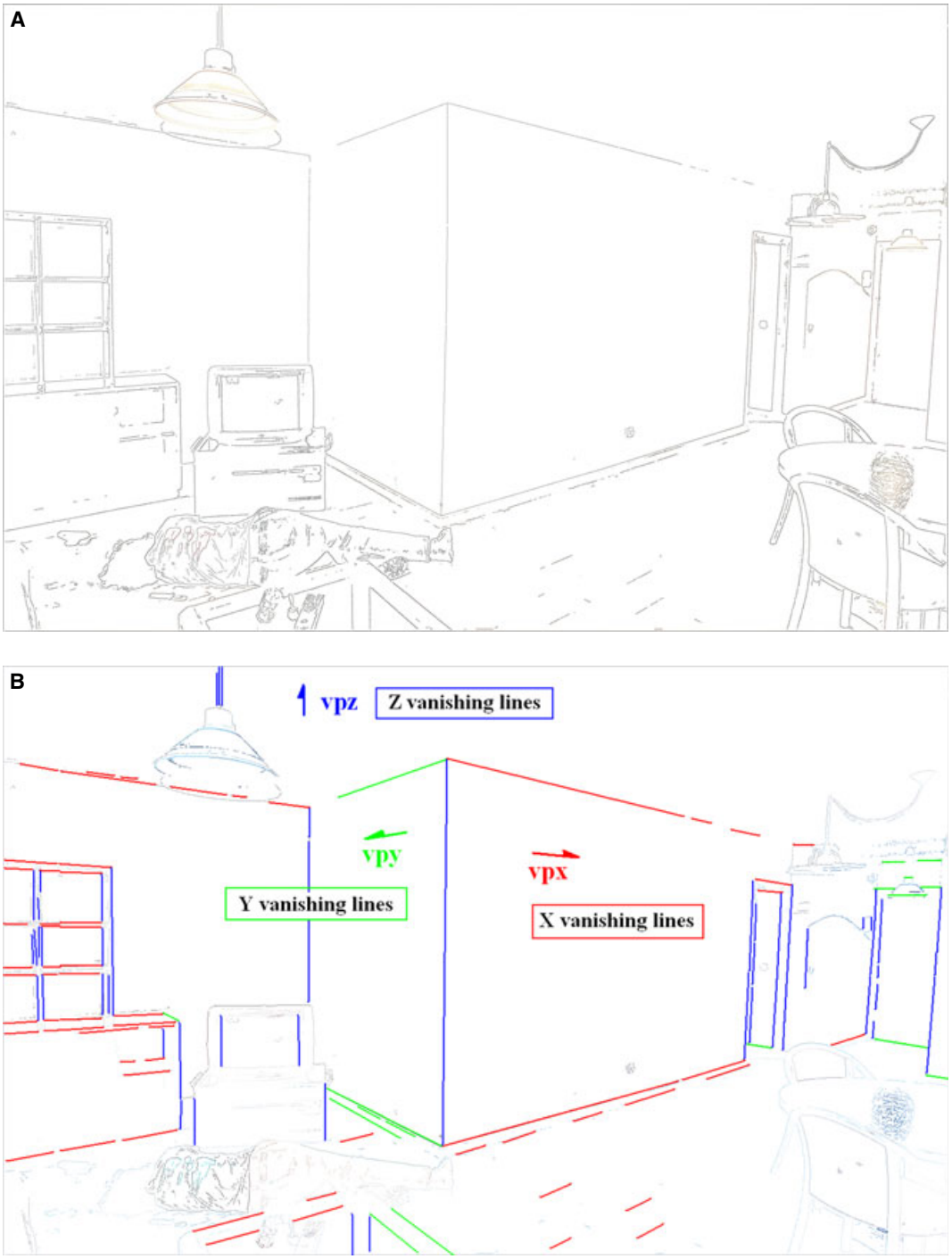

FIG8—*Case study 2: (A). Automatic straight line extraction: Canny + Burns. (B). Automatic clustering of vanishing lines according to the main directions of the crime scene (X,Y,Z).*

resolution of 5 mm was set up for a mean distance of 5 m. The laser scanner was completely leveled using its dual axis compensator to define the vertical axis direction without ambiguity. Likewise, range dataset were acquired from a unique station to eliminate any alignment error. These reference measurements could be considered free of error because the range distance was obtained with millimetric accuracy. Finally, in relation to the results, the discrepancies and the confidence intervals obtained lived up to forensic officers' expectations because the final average difference was around 0.02 m. Nevertheless, the results could have been even better considering that the measurement L_2 contains a higher standard deviation due to the particular interpretation of head and feet in the image by the operators.

Summary and Conclusions

The research project described in this paper has established that the forensic terrestrial photogrammetry from a single image has serious potential for aiding scientific police work. The approach supported by the software sv3DVision (31) has been evaluated by

TABLE 6—*Case study 2: statistics of features extraction and vanishing points coordinates in pixels.*

Vanishing Lines Clustering Outliers in Vanishing Lines	5 Segments Clustered as "Outliers"		
	72 Segments in *X* direction	26 Segments in *Y* direction	67 Segments in *Z* direction
Vanishing Points 2° Iteration	vpx	vpy	vpz
x	3762.2	16.8	782.4
y	923.8	860.4	40932.6
σ_{xx}	0.1	0.1	0
σ_{yy}	0	0.1	0.1

TABLE 7—*Case study 2: external camera parameters.*

External Parameters (Units: Degrees, m)		Deviations (Units: Degrees, m)	
Axis: 38.38°	*X*: −2.06	σ_{Axis}: 0.2°	σ_X: 0.01
Tilt: 87.36°	*Y*: −2.78	σ_{Tilt}: 0.3°	σ_Y: 0.01
Swing: 180.98°	*Z*: 1.51	σ_{Swing}: 0.04°	σ_Z: 0.01

a number of police officers, forensic scientists, and forensic educators who usually work with computerized investigation techniques, and their response has been very favorable. The fact that the sv3DVision is a true dimensional analyzer and three-dimensional

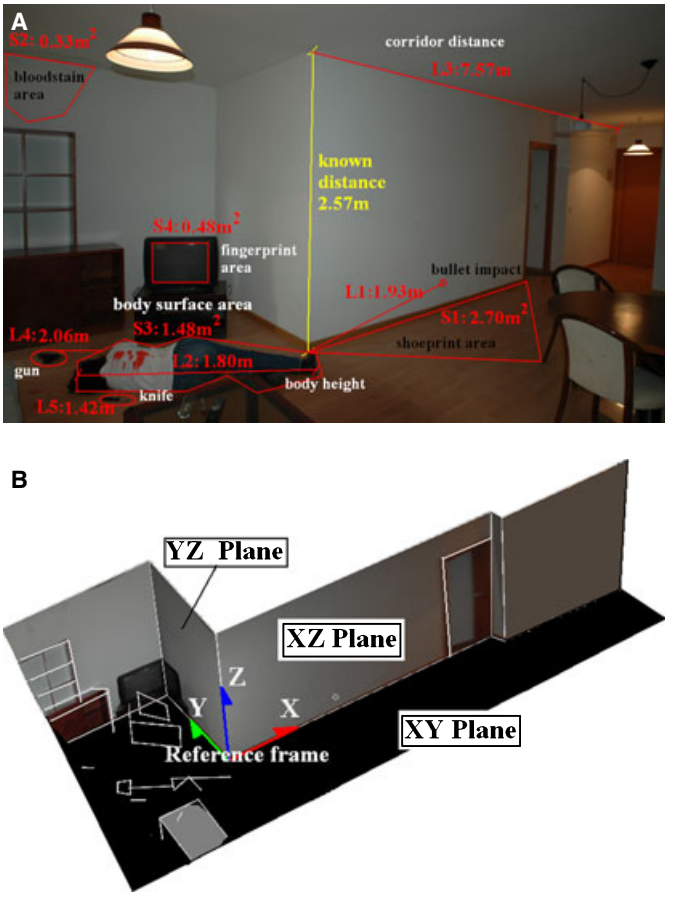

FIG. 9—*Case study 2. (A). Dimensional analysis. Measurements in meters averaged over each operator's measurements. (B). 3D reconstruction and visualization.*

TABLE 8—*Case study 2: dimensional analysis performed by three different operators measuring each dimension 10 times.*

Operator Test Distances (m)	1 Mean Measured Distance	2 Mean Measured Distance	3 Mean Measured Distance
*L*1	1.93	1.94	1.93
*L*2	1.79	1.81	1.81
*L*3	7.56	7.58	7.57
*L*4	2.06	2.06	2.07
*L*5	1.42	1.43	1.42
Test Areas (m^2)			
*S*1	2.70	2.69	2.71
*S*2	0.31	0.34	0.33
*S*3	1.47	1.49	1.48
*S*4	0.47	0.49	0.48

reconstructor of the real scene affords the opportunity to extract whatever metric information (that is, angles, distances, coordinates or surfaces areas), from a single image, could be crucial during forensic analysis.

According to the most novel aspects, the following developments could be outlined:

- The use of a single image together with amateur cameras constitutes a noninvasive technique which allows us to obtain the geometry of the crime scene (shape, size, and dimensions) even when the object of interest is inaccessible.
- Compared with other geomatic approaches, several favorable aspects could be outlined: from its low cost and its high level of automation, to its utility for users with no experience in photogrammetry and the quality of the results obtained, which have reached an average accuracy of 2 cm.
- From the scenarios presented, it should be clear that combined perspective geometries provided by other independent oblique images could serve not only to provide a dimensional analysis of the crime scene but also to fill missing information as well as to strengthen geometry using redundant information.
- An automatic estimation of internal camera parameters from single images has been incorporated. Particularly, radial lens distortion parameters are estimated from small features such as mini-segments together with vanishing point constraints. Nevertheless, better results could be obtained if the camera is calibrated previously.
- The implemented method incorporates a quality control of the measurements obtained. Particularly, error propagation is applied

TABLE 9—*Case study 2: reference measurements, mean measurements, their discrepancies, standard deviations, and confidence intervals, in meters.*

	Reference Distances	Mean Measured Distances	Mean Discrepancies	Standard Deviation	Confidence Intervals
Test Distances (m)					
*L*1	1.92	1.93	$\delta'_{L1} = -0.01$	$S_{\delta L1} = 0.01$	(1.90, 1.94)
*L*2	1.77	1.80	$\delta'_{L2} = -0.03$	$S_{\delta L2} = 0.02$	(1.73, 1.81)
*L*3	7.55	7.57	$\delta'_{L3} = -0.02$	$S_{\delta L3} = 0.01$	(7.53, 7.57)
*L*4	2.05	2.06	$\delta'_{L4} = -0.01$	$S_{\delta L4} = 0.01$	(2.03, 2.07)
*L*5	1.41	1.42	$\delta'_{L5} = -0.01$	$S_{\delta L5} = 0.01$	(1.39, 1.43)
	Reference Areas	Mean Measured Areas	Mean Discrepancies	Standard Deviation	Confidence Intervals
Test Areas (m^2)					
*S*1	2.68	2.70	$\delta'_{S1} = -0.02$	$S_{\delta S1} = 0.01$	(2.66, 2.70)
*S*2	0.29	0.33	$\delta'_{S2} = -0.04$	$S_{\delta S2} = 0.02$	(0.25, 0.33)
*S*3	1.45	1.48	$\delta'_{S3} = -0.03$	$S_{\delta S3} = 0.02$	(1.41, 1.49)
*S*4	0.45	0.48	$\delta'_{S4} = -0.03$	$S_{\delta S4} = 0.02$	(0.41, 0.49)

based on the law of variance-covariance matrix, while confidence intervals are used to provide probability statements.

According to the most critical aspects, this approach is successful in specific domains where the following assumptions have to be considered:

- The method is applicable over scenes with strong geometric contents (that is, presence of structural planes and lines). For example, it is not valid for irregular and complex shapes with the presence of concave, convex, or curved forms.
- The images acquired have to be oblique with three vanishing points. So, if there are more vanishing points, only those related to the three main directions of the scene will be extracted. If these vanishing points are well defined more precision and reliability can be reached for the dimensional analysis and 3D reconstruction from a single image.
- In order to overcome the image-based modeling problem, the user must know some *a priori* information about the scene (for example, a distance together with some geometric constraints).

Acknowledgment

The authors wish to thank the Scientific Madrid Police (Spain) for its collaboration and sponsorship providing the different images and measurements of crime scenes. As a result, a technology transfer agreement has been signed between two organizations (Scientific Madrid Police and the University of Salamanca).

References

1. Granshaw SI. Bundle adjustment methods in engineering photogrammetry. Photogramm Rec 1980;10(56):181–207.
2. González-Aguilera D, Gomez-Lahoz J. Dimensional analysis of a crime scene from a single image. Proceedings of the IEEE, International Congress on Image and Signal Processing, Hainan, China, May 27–30. Washington, DC: IEEE Computer Society, 2008.
3. Pollefeys M, Koch R, Vergauwen M, Van Gool L. Hand-held acquisition of 3D models with a video camera. Proceedings of the IEEE 2nd International Conference on 3D Digital Imaging and Modeling, Ottawa, Ontario, Canada, October 4–8. Washington, DC: IEEE Computer Society, 1999.
4. Se S, Jasiobedzki P. Instant scene modeler for crime scene reconstruction. Proceedings of the IEEE Computer Society Conference on Computer Vision and Pattern Recognition, San Diego, California, June 25. Washington, DC: IEEE Computer Society, 2005.
5. CSVR. Crime scene virtual tour. http://www.crime-scene-vr.com/ (accessed August 24, 2009).
6. Vanezisa P, Vanezisa M, McCombea G, Niblettb T. Facial reconstruction using 3-D computer graphics. Forensic Sci Int 2000;108:81–95.
7. Rusinkiewicz S, Levoy M. QSplat: a multiresolution point rendering system for large meshes. Proceedings of the 27th Annual Conference on Computer Graphics and Interactive Techniques, New Orleans, Los Angeles, July 23–28. New York, NY: ACM Press/Addison-Wesley Publishing Co., 2000.
8. Bahmutov G, Popescu V, Mudure M. Efficient large scale acquisition of building interiors. Comput Graph Forum 2006;25(3):655–62.
9. Thalia MJ, Braunb M, Markwaldera ThH, Brueschweilerb W, Zollingera U, Naseem J, et al. Bite mark documentation and analysis: the forensic 3D/CAD supported photogrammetry approach. Forensic Sci Int 2003; 135:115–21.
10. El-Hakim SF, Brenner C, Roth G. A multi-sensor approach to creating accurate virtual environments. ISPRS-J Photogramm Remote Sens 1998;6(53):379–91.
11. Popescu V, Sacks E, Bahmutov G. The model camera: a hand-held device for interactive modeling. Proceedings of the 4th International Conference on 3-D Digital Imaging and Modeling, Alberta, Canada, October 6–10. Washington, DC: IEEE Computer Society, 2003.
12. van den Heuvel FA. 3D reconstruction from a single image using geometric constraints. ISPRS-J Photogramm Remote Sens 1998;53(6):354–68.
13. Burns JB, Hanson AR, Riseman EM. Extracting straight lines. IEEE Trans Pattern Anal Mach Intell 1986;8(4):425–55.
14. Tuytelaars T, Van Gool L, Proesmans M, Moons T. The cascaded Hough transform as an aid in aerial image interpretation. Proceedings of the 6th International Conference on Computer Vision, Bombay, India, January 4–7. Washington, DC: IEEE Computer Society, 1998.
15. Hough PVC. Methods and means for recognizing complex patterns. U.S. Patent No. 3069654, 1962.
16. Liebowitz D, Criminisi A, Zisserman A. Creating architectural models from images. Comput Graph Forum 1999;18(3):39–50.
17. Almansa A, Desolneux A, Vamech S. Vanishing point detection without any a priori information. IEEE Trans Pattern Anal Mach Intell 2003;25(4):502–7.
18. Remondino F, Roditakis A. Human figures reconstruction and modeling from single images or monocular video sequences. Proceedings of the 4th International Conference on 3-D Digital Imaging and Modeling, Banff, Canada, October 6–10. Washington, DC: IEEE Computer Society, 2003.
19. Canny JF. A computational approach to edge detection. IEEE Trans Pattern Anal Mach Intell 1986;8(6):679–98.
20. Fischler MA, Bolles RC. Random sample consensus: a paradigm for model fitting with applications to image analysis and automated cartography. Commun ACM 1981;24(6):381–95.
21. Hartley R, Zisserman A. Multiple view geometry in computer vision. Cambridge: Cambridge University Press, 2000.
22. Barnard ST. Interpreting perspective images. Artif Intell 1983;21(4): 435–62.
23. Domingo-Preciado A. Investigación sobre los métodos de estimación robusta aplicados a la resolución de los problemas fundamentales de la Fotogrametría. [dissertation]. Santander: University of Cantabria, 2000.
24. Aguilera DG, Lahoz JG, Finat J. A new method for vanishing points detection in 3D reconstruction from a single view. Proceedings of the International Archives of Photogrammetry, Remote Sensing and Spatial Information Sciences, Commission V, Venice, Italy, Aug 22–24. Netherlands: ISPRS Archives, 2005.
25. Bräuer-Burchardt C, Voss K. Robust vanishing point determination in noisy images. Proceedings of the 15th International Conference on Pattern Recognition, Barcelona, Spain, September 3–7. Washington, DC: IEEE Computer Society, 2000.
26. Grammatikopoulos L, Karras GE, Petsa E. Camera calibration approaches using single images of man-made objects. Proceedings of the 19th CIPA International Symposium, Antalya, Turkey, 30 September–4 October. Netherlands: ISPRS Archives, 2003.
27. Caprile B, Torre V. Using vanishing points for camera calibration. Int J Comput Vis 1990;4(2):127–40.
28. Cipolla R, Drummond T, Robertson D. Camera calibration from vanishing points in images of architectural scenes. Proceedings of the British Machine Vision Conference, Nottingham, UK, September 13–16. Malvern, Worcs, UK: British Machine Vision Association, 1999.
29. Sturm PF, Maybank SJ. A method for interactive 3D reconstruction of piecewise planar objects from single images. Proceedings of the British Machine Vision Conference, Nottingham, UK, September 13–16. Malvern, Worcs, UK: British Machine Vision Association, 1999.
30. Mikhail EM, Ackermann F. Observations and least squares. New York: University Press of America, 1976.
31. Aguilera DG, Lahoz JG. sv3DVision: didactical photogrammetric software for single image-based modeling. Proceedings of the International Archives of Photogrammetry, Remote Sensing and Spatial Information Sciences, Commission VI, Tokyo, Japan, June 27–30. Netherlands: ISPRS Archives, 2006.

Additional information and reprint requests:
Diego Gonzalez-Aguilera, Ph.D.
Department of Cartographic and Land Engineering
University of Salamanca
50, Hornos Caleros
05003 Avila
Spain
E-mail: daguilera@usal.es